

# Aerodynamic Design and Analysis of a Blended Wing Body UAV Configuration

Swarna Mayuri Kumar  
M.Tech Scholar  
Mechanical Department  
Birla Institute of Technology and Science, Pilani  
India

**Abstract**—The current work is an Aerodynamic design study of a Blended Wing Body (BWB) Unmanned-Aerial-Vehicle (UAV). Trade studies are carried out to establish the aerodynamic design parameters based on the Design requirements. The traditional sizing and trade study methods were adopted to incorporate the characteristics of the BWB platform, further, the aerodynamic performance of the UAV can be increased by the implementation of a morphing design or an adaptive design.

On a BWB platform, a CFD-aided analysis of the morphing winglet concept is shown and explored. Three distinct configurations are computationally investigated in cruise flying conditions, at various angles of attack, using the winglet cant angle as the morphing parameter. The configurations are compared in terms of aerodynamic efficiency to determine the best setup for each of the BWB mission's pre-defined flight segments. The best configuration is then compared to the baseline configuration to determine the aerodynamic performance benefits of the morphing winglet idea. It is found that the drag coefficient is reduced at a high angle of attack with winglet configuration which also increases the lift to drag ratio. The addition of winglets to morphable wings improved the vehicle's aerodynamic performance. CFD analysis predicts the increase in the aerodynamic efficiency of the wing when the BWB vehicle is designed with a morphable winglet.

**Keywords**—Blended Wing Body (BWB), Unmanned Aerial Vehicle (UAV), Morphing Winglet, Aerodynamic Design, Computational Fluid Dynamics.

## I. INTRODUCTION

The Blended Wing Body (BWB) is a tailless design that merges the wing and fuselage and was originally intended as a unique platform for high-speed subsonic commercial airliners toward the end of the twentieth century [1, 2]. It consists of the main section (center body or fuselage) and an outer segment (wing), with the blending area in between, where the center body seamlessly merges (blends) into the wing geometry (Fig. 1). It has various advantages, including a low wetted area to internal volume ratio, the ability to distribute elliptic lift, a smooth changing cross-section distribution, and sufficient room for engine installation on the top of the airframe, to name a few. Cabin pressurization, passenger safety, and evacuation are some of the most essential difficulties of the BWB concept.

The BWB is a truly unique arrangement. With its benefits (improved aerodynamic efficiency and internal volume), it has the potential to improve the performance and operational requirements of aircraft that operate at low subsonic speeds,

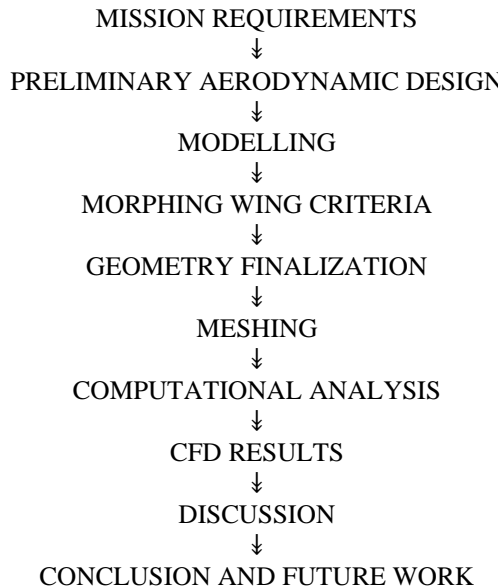
particularly in the incompressible flow domain, as most UAVs do.

The Aerodynamic design and analysis research of a BWB UAV is described in this paper. The mission specifications are like those of a standard surveillance UAV, as specified in [46].

## II. CONCEPTUAL DESIGN METHODOLOGY

A traditional sizing methodology is used for the conceptual design procedure outlined in this paper, which blends classic aircraft and UAV pre-sizing methodologies with computational simulations.

The Flow Chart depicts the conceptual design tool's roadmap.



### A. Mission Requirements

The defining of the aerial vehicle's mission requirements is the initial stage in aerodynamic design research. That is the operational requirements for payload weight, flight endurance, and flying speeds which correspond to a typical surveillance situation for UAVs [7,10,11].

Based on trade studies and comparisons of UAVs intended with similar mission requirements and planform the following performance specifications are listed below for the initial sizing and design of the BWB UAV to be versatile and competitive as a surveillance platform

- Payload 3 kg
- Endurance 4 hours
- Climb to an altitude of 3,000 meters (sea level) for aerial surveillance.
- Counter gusts/crosswind speeds of 20 meters/second.
- Maximum velocity of operation of 35 meters/second

#### B. Estimating the Gross Take-off weight of the UAV

Calculating the first weight estimate is the first stage in the layout design study. The GTOW of a UAV is calculated by adding the payload weight  $W_p$ , fuel weight  $W_f$ , and empty weight  $W_e$ .

The payload weight refers to the entire weight of onboard electronic and surveillance equipment, and it must be sufficiently high to account for radios, optical and infrared sensors, and onboard computers.

The UAV target weight is approximated using historical trends and statistical data for operating aircraft with similar needs in this first design stage [7,11]. More specifically, the data from [7] were used. The GTOW of the BWB UAV was assumed to be around 15kg.

i.e.,  $GTOW = 15 \text{ Kg}$  to carry a payload of approximately 3kg to 4kg

#### C. The BWB Baseline Design

Geometry was created, considering some guidelines from other BWB references, such as NASA's X-48B.

#### D. Statistical analysis and initial sizing

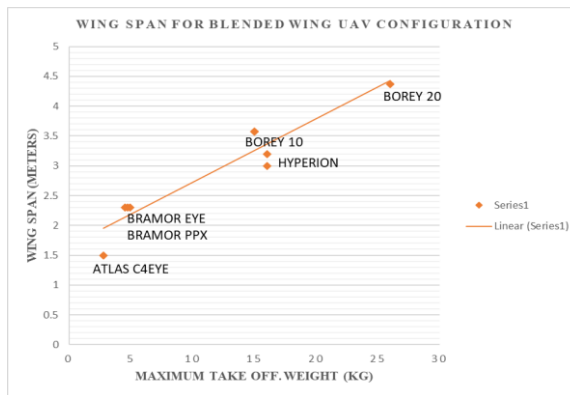


Fig 1. The statistical curve for wingspan selection

According to the curves obtained from the statistical data as shown in figure 1 a total span of 3.2 meters is chosen for an MTOW of 15 kg.

#### E. Airfoil selection

Airfoils were chosen to meet BWB specifications i.e., high t/c, negative camber for pitch stability, and high L/D for low Reynolds numbers. S5010 is chosen for the wing considering and AS5016 Airfoil is chosen for the body section of the BWB as it is just a modification of the Low Reynolds number Selig airfoil with a Maximum thickness of 16 % as the central body

of the BWB houses the payload and other components required for light.

#### F. The final model of the BWB UAV with the winglets

The rest of the geometric parameters as given in table 1 were selected according to the design requirements [8], considering typical values for other BWB models and near-optimum values. Once all the design features were defined, an iterative shape refinement process was performed using the CAD tool CATIA, to smooth the outer surface and eliminate bumps and irregularities.

TABLE I. GATHERS SOME GEOMETRIC CHARACTERISTICS OF THE BWB MODEL OBTAINED.

PARAMETER	VALUE
Wingspan, $b$	3.2 m
Wing Area, $S$	1.5678 m <sup>2</sup>
Mean Aerodynamic Chord, MAC	0.961
Mean Geometric Chord, MGC	0.655
Aspect Ratio, AR	3.6
Taper Ratio	0.083
Dihedral Angle, $\Gamma$	6°
Total Length, $L_{BWB}$	1.734
Fuselage Length, $L_f$	1.609
Total Height, $h_{BWB}$	0.326
Fuselage Height, $H_f$	0.253
Leading Edge Sweep Angle, $A_{LE}$	63° (Fuselage), 39° (Wing)

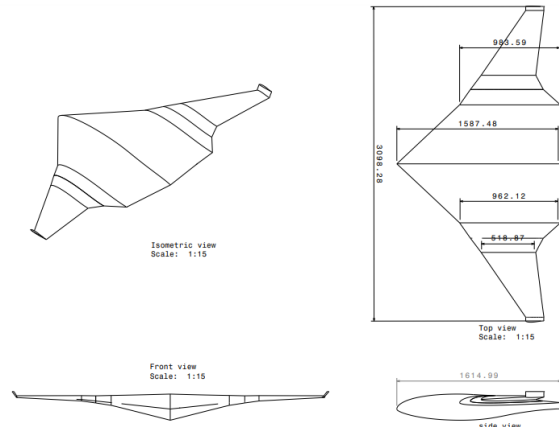


Fig 2. shows the final design layout and configuration

#### III. MORPHING WING CRITERIA

Small wing-like structures at the end of the wing are called winglets, it improves the aerodynamic efficiency of the wing by reducing the lift-induced drag caused by the vortices at the tips of the wing.

The total Drag of an aircraft, or a wing is equal to the sum of parasite drag, lift-induced drag, and wave drag. Winglets are aerodynamically viable only when the reduction of lift-induced drag is larger than the increment in parasite drag, Today's 3 to 5% difference in fuel economy is due to the use of fixed winglets optimized for cruising flight. We can sustain a 5% fuel reduction throughout the flight if we alter the cant angle throughout the flight." Allowing the winglet to completely flatten will also provide additional lift at low speeds. Such winglets are called morphing winglets or

morphlets and shape-memory alloys (SMAs) are mainly used for such purposes.

The winglet dimensions were determined during the trade-off. The same airfoil used for the wing is used for the winglet, in general sizing, the winglet span length is between 0.1 to 0.2 of the wing semi span length, hence a winglet span of 0.17m is fixed.

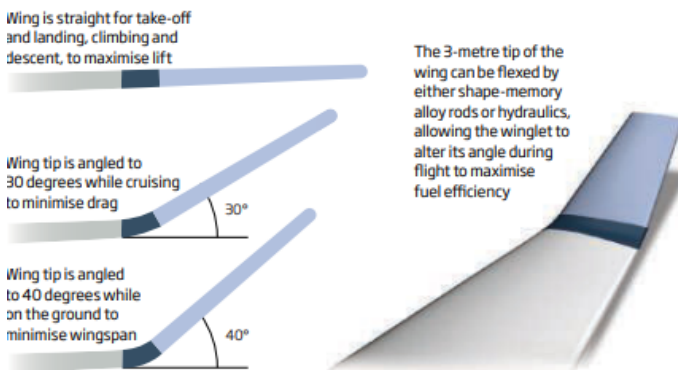


Fig 3. The morphing of Wing shown at various cant angles

#### IV. NUMERICAL ANALYSIS OF DRAG REDUCTION

The performance of aircraft without winglets and with winglets is measured by comparing the aerodynamic efficiency of the aircraft with two different configurations. Aerodynamic efficiency is defined as the ratio between the lift force to the drag force or the ratio between the coefficient of lift to the coefficient of drag.

$$E = L/D = C_L/C_D$$

Where

E - Aerodynamic Efficiency

L - Lift in N

D - Drag in N

$C_L$  - Coefficient of Lift

$C_D$  - Coefficient of Drag

By calculating the aerodynamic efficiency, the percentage of drag reduction can be calculated which will help us to conclude that having a winglet at BWB is beneficial.

#### V. COMPUTATIONAL ANALYSIS AND RESULT DISCUSSION

This paper uses computational fluid dynamics to investigate the morphing winglet idea on a BWB platform. The baseline wing and winglet designs are based on an existing BWB platform, whereas the morphing parameter is the winglet cant angle. By solving the RANS equations, two distinct cant angle combinations one at a cant angle of zero degrees and the other at an angle of 80 degrees are computationally analyzed at various angles of attack and compared with the model without a winglet.

Simulation is performed with the ANSYS workbench tool, however different tools in the ANSYS workbench is used for pre-processing, solving, and post-processing. Wing design CAD is imported into the design modeler tool of the ANSYS workbench, and the surrounding environment is created in the

tool as shown in figure 10. The next step involves discretization of fluid domain mainly named meshing. Mesh is generated for the fluid model in ANSYS Mesher. The tetrahedral patch conforming method is used for mesh generation and inflation layers are created around the wing. 10 inflation layers are generated around the wing to get good  $y^+$  values.

Simulation setup, solving, and post-processing are done in the Ansys CFX tool, where meshed geometry is imported into the tool and appropriate boundary conditions are defined. Far from the wing, velocity inlet is defined, however, all other environment faces opening boundary condition is defined with 0 Pa gauge static pressure. Simulations are performed with 5 different angles of attack

Following input parameters were defined for the simulation.

#### Input parameters

Fluid: Air at 25 [°C]

Turbulence Modelling: Spalart-Allmaras modelling

Thermodynamics: Isothermal

Boundary Conditions:

Inlet: Velocity =30 [m/s]

Opening: Static Pressure = 0 [Pa] (Gauge Pressure)

Angle of Attack: [-12, -6, 0, 6, 12] degrees

The same simulation settings and boundary conditions are used throughout the analyses for consistency in results.

#### A. Case I: Model without winglet

This is the reference case and other winglet designs are compared with respect to this, the tetrahedral mesh generated is shown in figure 4

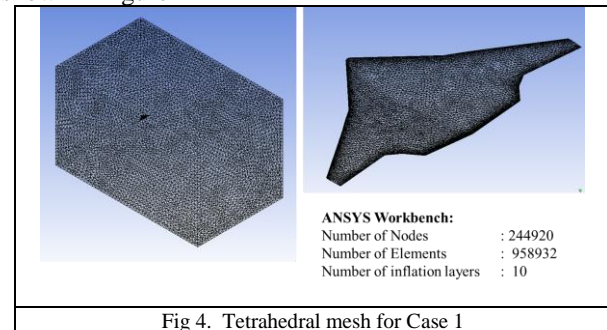


Fig 4. Tetrahedral mesh for Case 1

#### 1) Simulation Results

##### 1) -12 degrees AOA without winglet

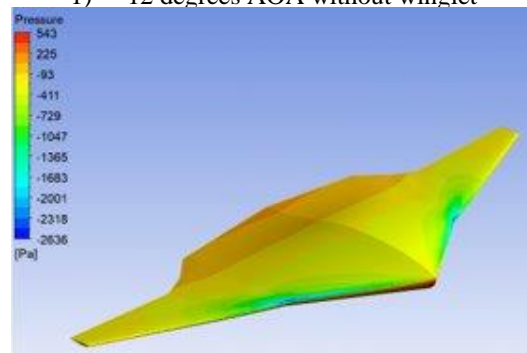


Fig 5. Pressure contour over the wing

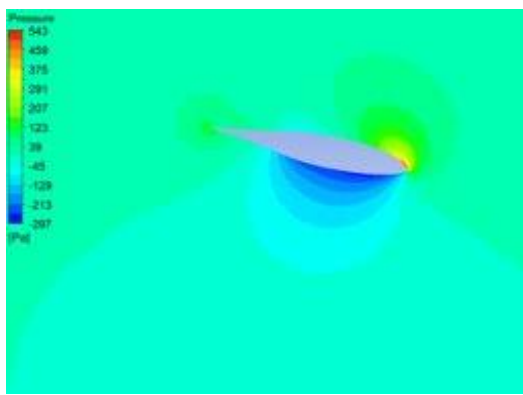


Fig 6. Pressure contour on the middle plane

2) 12 degrees AOA without winglet

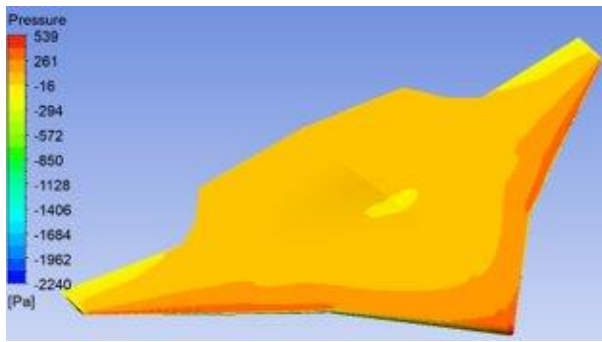


Fig 7. Pressure Contour over Wing

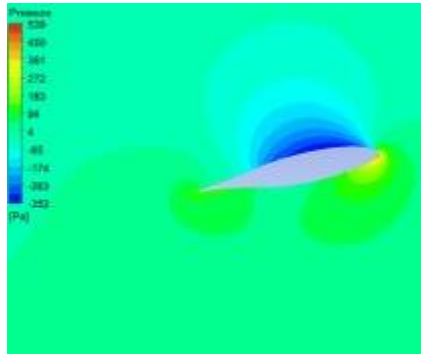


Fig 8. Pressure contour on the middle plane

Lift and drag coefficient are calculated using following formula

$$Cl = \frac{Lift}{0.5 \cdot \rho \cdot S_1 \cdot u^2}, S_1 = 2.38 \text{ m}^2$$

$$Cd = \frac{Drag}{0.5 \cdot \rho \cdot S_2 \cdot u^2}, S_2 = 0.297 \text{ m}^2$$

Simulation results as shown in table 2 below indicate that with an increased angle of attack the lift increases. The highest lift is observed for a +12-degree angle of attack. It is also observed that lift and drag are not symmetric to the angle of attack as expected because the wing also is not symmetric. The lowest drag is observed for the 0-degree case.

TABLE II: LIFT AND DRAG FOR WITHOUT WINGLET CASE

AOA	Drag [N]	Lift [N]	Cd	Cl	L/D
-12	123.736	-701.286	0.785	-0.553	-5.66759876
-6	39.896	-349.942	0.253	-0.276	-8.77135552
0	16.418	103.156	0.104	0.081	6.28310391
6	41.392	559.89	0.263	0.441	13.52652687
12	122.04	932.466	0.774	0.735	7.6406588
18	290.322	1026.054	1.842	0.808	3.534193068
25	445.922	1029.064	2.829	0.811	2.307721978

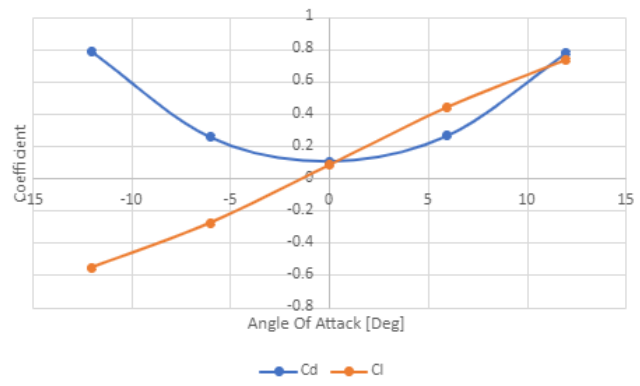


Fig 9. Cl and Cd Coefficient with respect to Angle of attack

B. Case II: Model with winglet canted at an angle of zero degrees to the wing

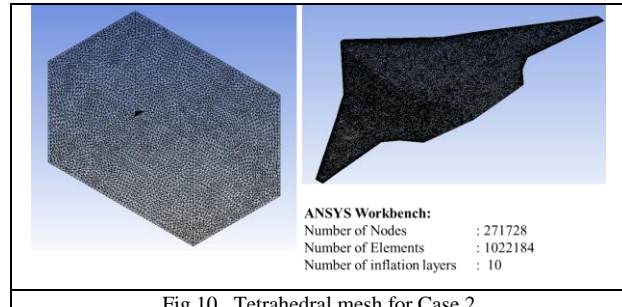


Fig 10. Tetrahedral mesh for Case 2

1) Simulation Results

a) -12 degrees AOA with winglet at a cant angle of 0 degrees

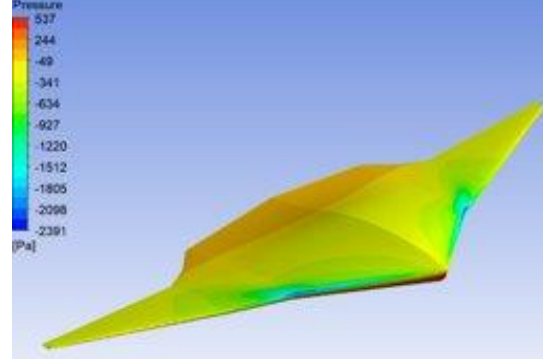


Fig 11. Pressure Contour over Wing

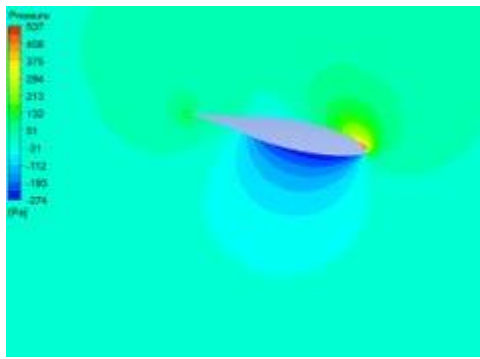


Fig 12. Pressure contour on the middle plane

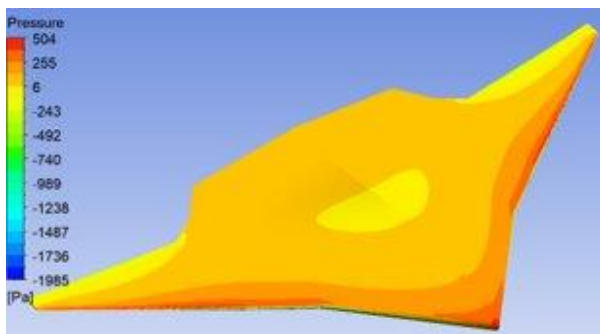


Fig 13. Pressure Contour over Wing

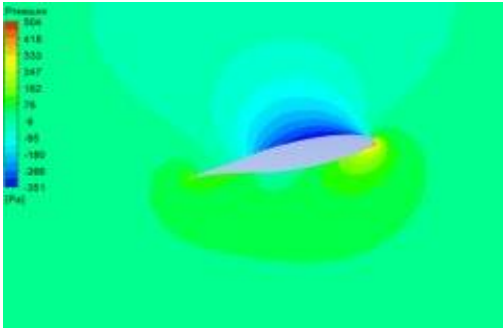


Fig 14. Pressure contour on the middle plane

It can be clearly seen from the lift and drag data given in table 3 that at a higher angle of attack lift has improved. This indicates that the performance of the wing has improved with winglet design.

TABLE III: LIFT AND DRAG FOR WITH WINGLET 0 DEGREE CASE

A	Drag [N]	Lift [N]	Cd	Cl	L/D
-12	136.08	-688.178	0.863	-0.542	-5.05716
-6	44.212	-362.936	0.28	-0.286	-8.20899
0	17.246	102.412	0.109	0.081	5.938305
6	43.162	572.672	0.274	0.451	13.26797
12	133.638	919.136	0.848	0.724	6.877804
18	278.982	942.82	1.77	0.743	3.379501
25	437.886	1016.44	2.778	0.801	2.321243

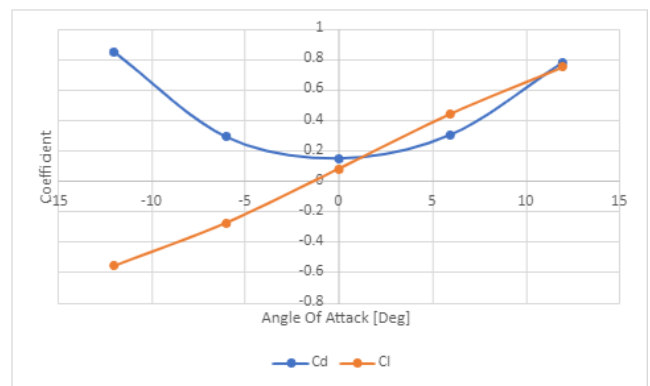


Fig 15. Cl and Cd Coefficient with respect to Angle of attack

**C. Case III: Model with winglet canted at an angle of 80 degrees to the wing**

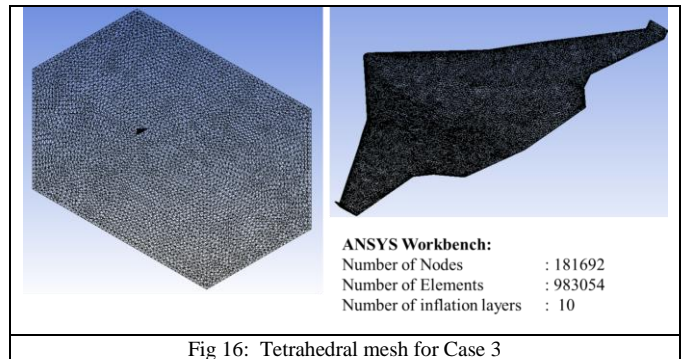


Fig 16: Tetrahedral mesh for Case 3

**1) Simulation Results**

a) -12 degrees AOA cant angle with winglet canted at 80 degrees

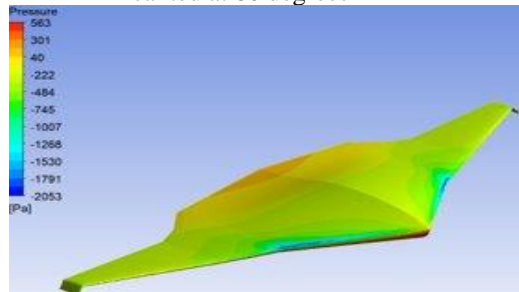


Fig 17. Pressure contour over the wing

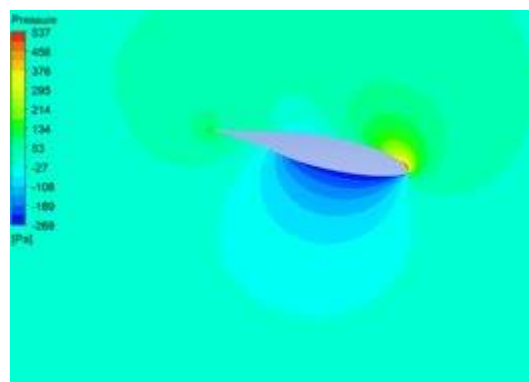


Fig 18. Pressure contour over the middle plane

b) 12 degrees AOA cant angle with winglet canted at 80 degrees

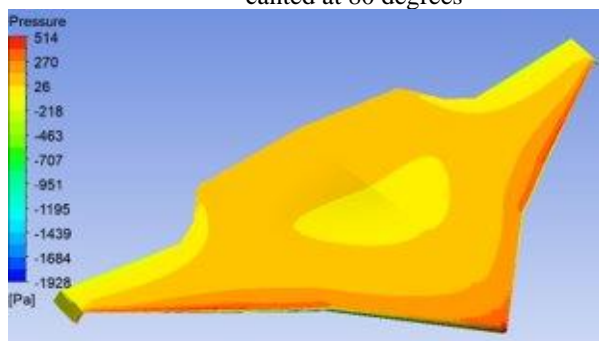


Fig 19. Pressure contour over the wing

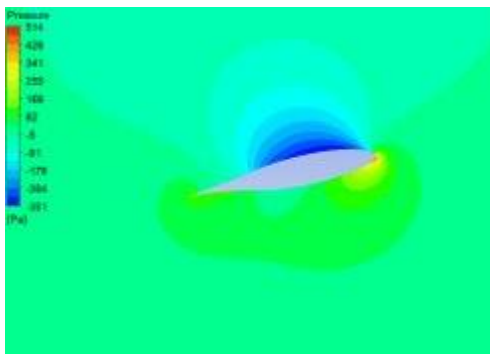


Fig 20. Pressure contour over the middle plane

It can be clearly seen in the lift and drag data that at a higher angle of attack, the lift has improved. This indicates that the performance of the wing has improved with winglet design. It is also observed that rotating winglets by 80 degrees has reduced the drag with an increase in the lift. It has certainly improved the performance of the wing.

TABLE IV: LIFT AND DRAG FOR WITH WINGLET 80 DEGREE CASE

AOA	Drag [N]	Lift [N]	Cd	C <sub>l</sub>	L/D
-12	135.046	-732.766	0.857	0.577	-5.42605
-6	44.684	-367.434	0.283	-0.29	-8.22294
0	17.472	107.486	0.111	0.085	6.1519
6	43.722	579.532	0.277	0.457	13.25493
12	132.158	939.606	0.838	0.74	7.109717
18	307.278	1076.382	1.949	0.848	3.502958
25	589.918	1434.802	3.742	1.131	2.432206

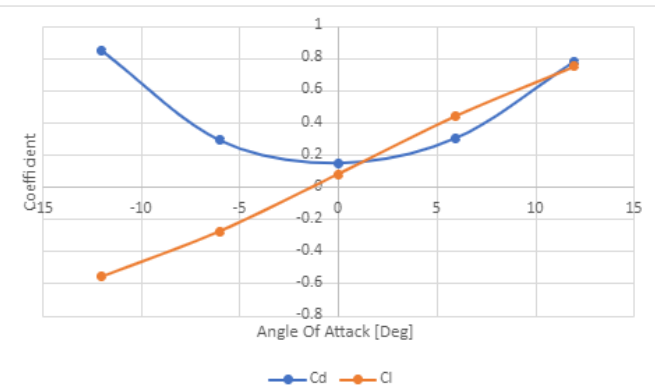


Fig 21. C<sub>l</sub> and C<sub>d</sub> Coefficient with respect to Angle of attack

#### D. Comparison of lift and drag coefficients for all the three cases

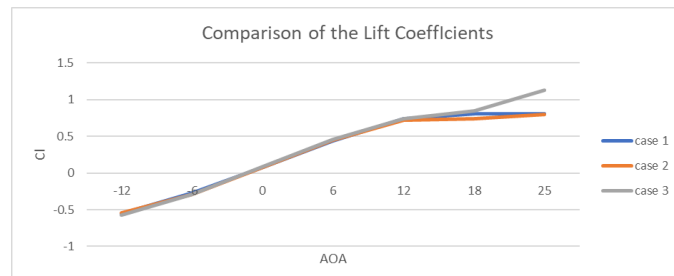


Fig 22. Comparing the lift coefficients for the three cases

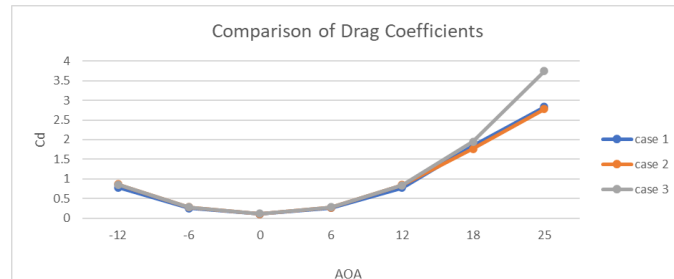


Fig 23. Comparing the drag coefficients for the three cases

#### VI. CONCLUSION AND FUTURE WORK

On a BWB platform, a CFD-aided analysis of the morphing winglet concept is shown and explored. Three distinct configurations are computationally investigated at various angles of attack, using the winglet cant angle as the morphing parameter. The configurations are compared in terms of aerodynamic efficiency to determine the best setup for each of the BWB mission's pre-defined flight segments. The best configuration is then compared to the baseline configuration to determine the aerodynamic performance benefits of the morphing winglet idea. It is found that a high angle of attack with winglet configuration also increases the lift to drag ratio. It is also seen from the L/D ratio and by comparing the Lift and drag coefficient graphs for all the three cases, that the aerodynamic efficiency of the BWB with a Morphable winglet has improved over that of the configuration without a winglet but further improvements in the results can be brought about by the improvement in the design and optimization of the winglet which should be considered as a future work.

More distinct cant angle combinations can be considered apart from the present two cases to prove the efficiency of wing morphing using a winglet further. It is also

recommended that the UAV be modeled after sufficient structural Design and analysis and wind tunnel experiments can be performed which can give data to validate the computational results. Finally, experimental confirmation of the morphing winglet arrangement is recommended

#### ACKNOWLEDGMENT

I express my gratitude to my mentors Mr. Athappan M and Mr. K Subash for providing me means of attaining my most cherished goals. I also extend my gratitude to my Professor Mr. Pardha Sarathy Gurugubelli Venkata for giving me an opportunity to carry out this project, along with purposeful guidance and moral support extended to me throughout the duration of the project work

Finally, I thank the God Almighty, my family, and friends who showed immense support throughout my journey in the completion of this project.

#### REFERENCES

- [1] Panagiotou, P.; Fotiadis-Karras, S.; Yakinthos, K. (2017). *Conceptual design of a Blended Wing Body MALE UAV. Aerospace Science and Technology*, (), S1270963817315870-. doi:10.1016/j.ast.2017.11.032
- [2] Marks, Paul (2009). 'Morphing' winglets to boost aircraft efficiency. *New Scientist*, 201(2692), 22–23. doi:10.1016/S0262-4079(09)60208-6
- [3] Qin, N., Vavalle, A., Le Moigne, A., Laban, M., Hackett, K., Weinerfelt, P.: Aerodynamic considerations of blended wing body aircraft. *Prog. Aerosp. Sci.* 40, 321–343 (2004). doi:10.1016/j.paerosci.2004.08.001
- [4] Li, P., Zhang, B., Chen, Y., Yuan, C., Lin, Y.: Aerodynamic Design Methodology for Blended Wing Body Transport. *Chin. J. Aeronaut.* 25, 508–516 (2012). doi:10.1016/S1000-9361(11)60414-7
- [5] Lyu, Z., Martins, J.R.R.A.: Aerodynamic Design Optimization Studies of a Blended-Wing-Body Aircraft. *J. Aircr.* 51, 1604–1617 (2014). doi:10.2514/1.C032491
- [6] Engels, H., Becker, W., Morris, A.: Implementation of a multi-level optimisation methodology within the e-design of a blended wing body. *Aerosp. Sci. Technol.* 8, 145–153 (2004). doi:10.1016/j.ast.2003.10.001 .
- [7] Jean Koster., Alex Velazco., Claus-Dieter Munz., Ewald Kraemer., KC Wong., Dries Verstraete.: HYPERION UAV: An International Collaboration. In: 50th AIAA Aerospace Sciences Meeting including the New Horizons Forum and Aerospace Exposition 09 - 12 January 2012, Nashville, Tennessee
- [8] Roberto Merino-Martinez.: Design and analysis of the control and stability of a Blended Wing Body aircraft, Polytechnic University of Madrid (UPM)
- [9] J. E. Guerrero., M. Sanguineti., K. Wittkowski.: Variable cant angle winglets for improvement of aircraft flight performance. *Meccanica* (2020) 55:1917–1947. doi: 10.1007/s11012-020-01230-1
- [10] Vos, R., Geuskens, F.J.J.M.M., Hoogreef, M.F.M.: A New Structural Design Concept for Blended Wing Body Cabins. In: Proceedings of the 53rd AIAA/ASME/ASCE/AHS/ASC Structures, Structural Dynamics and Materials Conference, Structures, Structural Dynamics, and Materials and Co-located Conferences (2012). doi: 10.2514/6.2012-1998
- [11] Shim, H.J., Park, S.O.: Low-speed Wind-tunnel Test Results of a BWB-UCAV Model. *Procedia Eng.* 67, 50–58 (2013). doi:10.1016/j.proeng.2013.12.004
- [12] Austin, R.: Unmanned Aircraft Systems, UAVS design, Development and Deployment. Wiley, Chichester, West Sussex, United Kingdom (2010)